Nonconvulsive Epileptic Seizures Detection Using Multiway Data Analysis

Yissel Rodríguez Aldana
Universidad de Oriente
Center of Neuroscience and
Signals and Image Processing
Santiago de Cuba, Cuba
Email: yaldana@uo.edu.cu

Borbála Hunyadi
KU Leuven
Stadius Center for Dynamical Systems
Signal Processing and Data Analytics
Leuven, Belgium
Email: borbala.hunyadi@esat.kuleuven.be

Enrique J. Marañón Reyes
Universidad de Oriente
Center of Neuroscience and
Signals and Image Processing
Santiago de Cuba, Cuba
Email: enriquem@uo.edu.cu

Valia Rodríguez Rodríguez
Cuban Neuroscience Center
ICU-Ameijeiras Clinic Surgical Hospital
La Habana, Cuba
Aston University, United Kingdom.
Email: v.rodriguez@aston.ac.uk

Sabine Van Huffel
KU Leuven
Stadius Center for Dynamical Systems
Signal Processing and Data Analytics
IMEC, Leuven, BE
Leuven, Belgium
Email: sabine.vanhuffel@esat.kuleuven.be

***Abstract*—Nonconvulsive status epilepticus (NCSE) is observed when the patient undergoes a persistent electroencephalographic epileptic episode without physical symptoms. This condition is commonly found in critically ill patients from intensive care units and constitutes a medical emergency. This paper proposes a method to detect nonconvulsive epileptic seizures (NCES). To perform the NCES detection the electroencephalogram (EEG) is represented as a third order tensor with axes $frequency \times time \times channels$ using Wavelet or Hilbert–Huang transform. The signatures obtained from the tensor decomposition are used to train five classifiers to separate between the normal and seizure EEG. Classification is performed in two ways: (1) with each signature of the different modes separately, (2) with all signatures assembled. The algorithm is tested on a database containing 139 nonconvulsive seizures. From all performed analysis, Hilbert–Huang Tensors Space and assembled signatures demonstrate to be the best features to classify between seizure and non-seizure EEG.**

I. Introduction

Nonconvulsive status epilepticus (NCSE) is observed when the patient undergoes a persistent electroencephalographic epileptic episode without evident physical symptoms. The NCSE can be classified in two major categories: with coma/stupor and without coma/stupor (absence or focal epileptic seizures). The appearance of nonconvulsive epileptic seizures (NCES) in comatose or unresponsive patients' EEG is often associated with serious brain damage and a very poor prognosis [1]. The prompt recognition of patients at risk of suffering from NCSE is necessary in order to manage them accordingly and to provide the treatment when permanent brain damage can be still prevented.

The methods proposed for NCESs detection published until 2015 are summarized in a review paper by Ansari and Sharma [2]. This review pointed out that Support Vector Machines (SVM), Neural Networks (NN) and Linear Discriminant functions (LD) were the most widely used classifiers, while Wavelet Transform (WT), Entropy and nonlinear parameters were the most popular features to describe the NCES data.

This paper proposes a method to detect NCES based on multiway data analysis. The electroencephalogram (EEG) data is represented as a third order tensor in the way $A \in R^{(F \times T \times S)}$ with axes $frequency \times time \times channels$. Different $time \times frequency$ transforms may be used to construct such tensors. Although WT is a very popular tool in EEG analysis, here we propose to use the Hilbert-Huang Transform (HHT) as well, as it provides a more accurate definition of particular-events in the $time \times frequency$ space than WT and gives a better physical interpretation to the underlying EEG activity [3]. Multiway analysis is a very powerful tool in EEG analysis, as it can tackle spatial, temporal and spectral properties of the EEG at the same time. It has been shown that tensor decompositions of multiway EEG representations can extract seizure sources and accurately characterize the seizure pattern [4]. As such, this approach represents an elegant, simple, yet effective alternative to the extraction of large and heterogeneous feature sets. The signatures from the tensor decomposition will be used as features for training the seizure detector.

This work has been supported by the Belgian Development Cooperation through VLIRUOS (Flemish Interuniversity Council-University Cooperation for Development) in the context of the Institutional University Cooperation program with Universidad de Oriente.

The research leading to these results has received funding from the European Research Council under the European Union's Seventh Framework Programme (FP7/2007-2013) / ERC Advanced Grant: BIOTENSORS (no. 339804). This paper reflects only the authors' views and the Union is not liable for any use that may be made of the contained information.

ISBN 978-0-9928626-7-1

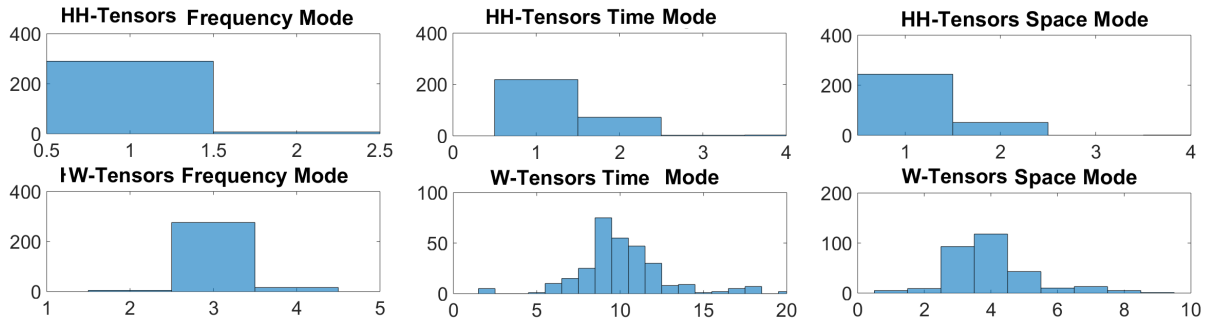

Fig. 1. Histograms for the Frequency, Time and Space Modes. LMLRA analysis of all training datasets. Axis X and Y represents the number of components and tensors respectively.

II. Material and Methods

A. Data Description

EEG data was collected as part of patients' clinical assessment at the Epilepsy Unit of the Cuban Neurological Restoration Center (CIREN) and at the Intensive Care Units (ICU) of Clinical Surgical Hospital Hermanos Ameijeiras, both in Havana City. Data was anonimized to be used in this study. In every case the electrodes were placed according to the 10-20 montage system. Since patients come from different hospitals, the acquisition protocol differs among the data. The number of recording electrodes vary from 8 to 19, with a sampling rate of 200 Hz. Our dataset includes 14 patients aged between 18 and 57 years old, with a total of 139 seizures (55 with coma/stupor); all of which are diagnosed as NCES by the neurophysiologist and neurologist. All procedures were reviewed and approved by the Ethical Committees of the CIREN and Hermanos Ameijeiras Hospital respectively.

B. Tensor formulation

To build the tensors, each EEG data channel was transformed to $time \times frequency$ domain using WT or HHT. The EEG signal was analysed in segments of 3s duration. The transformation was applied to each EEG channel at every segment, resulting in one $frequency \times time \times channels$ tensor per segment.

The WT decomposes a signal $x(t)$ into frequency subbands at different time scales. It convolves $x(t)$ with a mother wavelet function $\psi(n)$ dilated and scaled in the way,

$$x_w(a,b) = \frac{1}{\sqrt{|a|}} \int_{-\infty}^{\infty} x(t)\psi^*\left(\frac{t-b}{a}\right)dt \tag{1}$$

Where $()*$ indicates the complex conjugate, ψ is the analysing wavelet, a (>0) is the scale parameter and b is the dilation parameter [5]. For the transformation, the "Mexican Hat" mother wavelet was used [6], [4]. Since the NCES activity is below 5Hz, [7] five wavelet scales were computed, which correspond to 1-5 Hz frequencies, with 1 Hz resolution. The x_w matrices extracted from each channel are stacked into a tensor $A \in R^{(F \times T \times S)}$, further on W_Tensors, where F is the number wavelet scales, T is the number of time samples per segment and S is the number of EEG channels.

The HHT was proposed by Huang et al [8]. This transformation is performed in two steps: 1) obtain the Empirical Mode Decomposition (EMD) and 2) compute the Hilbert spectrum of the results from the previous step. EMD decomposes a signal in a set of intrinsic mode functions (IMF) and a residue. This residue is conventionally defined as the trend of the series.

By definition, an IMF meets two conditions: (i) for the entire data set, the number of extrema and the number of zero crossings must be either equal or differ at most by one and (ii) the mean at any point of the contour defined by interpolating the local maxima (upper envelope) and the contour defined by interpolating the local minima (low envelope) is zero [9]. The EMD can be described with the following equation,

$$x(t) = \sum_{k=1}^{n} imf_k(t) + r(t) \tag{2}$$

where imf_k is the k^{th} IMF of the signal, and r is the residue [8].

Once the IMFs are computed , they can be projected on a $frequency \times energy \times time$ space

$$x_{HH} = w \circ s \circ t \tag{3}$$

where $\circ$ means the matrix outer product, t is the time vector, w is the instantaneous frequency and s is the energy defined as

$$s(t) = a(t)^2 \tag{4}$$

a is instantaneous amplitude. Both $w$and s are $n \times t$ matrices where n is number of IMF. This space is obtained by computing the Hilbert transform and w as,

$$y_{imf_k}(t) = \frac{1}{\pi} P \int_{-\infty}^{\infty} \frac{imf_k(t)}{t - t_0} dt \tag{5}$$

and

$$w_{imf_k}(t) = \frac{d\theta_{imf_k}(t)}{dt} \tag{6}$$

respectively. P indicates the Cauchy principal value and θ_{imf_k} is the instantaneous phase. $y_{imf_k}(t)$ and $imf_k(t)$ form a complex conjugate pair that describes an analytic signal $z_{imf_k}(t)$,

$$z_{imf_k}(t) = imf_k(t) + jy_{imf_k}(t) = a_{imf_k}(t)e^{j\theta_{imf_k}(t)} \tag{7}$$

ISBN 978-0-9928626-7-1 © EURASIP 2017

where a_{imf_k} and θ_{imf_k} are defined as,

$$a_{imf_k}(t) = \sqrt{[imf_k(t)]^2 + [y_{imf_k}(t)]^2} \tag{8}$$

and

$$\theta_{imf_k}(t) = \arctan\left(\frac{y_{imf_k}(t)}{imf_k(t)}\right) \tag{9}$$

respectively.

To obtain the instantaneous $frequency \times time$ matrices $x_{HH_{2D}}(w,t)$ the amplitude elements were accumulated in the frequency subscripts at every time instant in the way,

$$x_{HH_{2D}}(w,t) = \sum_{k=1}^{n} s_k(w,t) \tag{10}$$

As for CWT the Hilbert spectrum was taken at 1-5 Hz. The $x_{HH_{2D}}(w,t)$ matrices were arranged as an $A \in R^{(F\times T\times S)}$ tensor, further on defined as HH_Tensors, where F indicates the 1-5 Hz frequency values, T the number of time samples and S the number of EEG channels.

The two tensor sets obtained, W_Tensors and HH_Tensors, were decomposed with the Canonical Polyadic Decomposition.

C. Tensor Decomposition

The Canonical Polyadic Decomposition (CPD) represents an $N^{th}-$ order tensor $X \in R^{(I_1\times I_2\times I_3\times\cdots\times I_N)}$ as the outer product of rank-1 tensors in the following way,

$$X = \sum_{r=1}^{R} b_r^{(1)} \circ b_r^{(2)} \circ \ldots \circ b_r^{(N)} \tag{11}$$

Where R is a positive integer and $b_r^{(1)} \in R^{I_1}, b_r^{(2)} \in R^{I_2}, \ldots, b_r^{(N)} \in R^{I_N}$ are nonzero vectors that express the N mode signature.

The tensor rank of X is equal to the minimal number of components R that generates an 'exact' CPD of X, where 'exact' means that there is equality at the Eq.11 [10]. However, in this application we are not interested in an exact reconstruction. In fact, we expect that additional unstructured noise contaminates the EEG data. Instead, we are looking for a good low rank approximation, which captures enough information about the seizure pattern for correct classification.

To estimate the number of components required to perform the decomposition, R values were estimated with the MatLab toolbox Tensorlab [11]. First, using the rankest function of Tensorlab, an upper bound of $R = 4$ and $R = 9$ was obtained for HH_tensors and W_tensors, respectively. Afterwards, these values were refined as follows: CPD and the low multilinear rank approximation (LMLRA) [12] were performed with increasing R, starting from $R = 1$, until the desired approximation was achieved. The desired approximation was defined in terms of the relative error (*relerr*), which was chosen here as 0.2. For CPD pseudorandom initialization and a Nonlinear Least Squares algorithm was used.

This procedure was performed for all training examples in the dataset. Therefore, for every segment, we obtained a rank value in each of the 3 modes (i.e. frequency, time and channel). Afterwards, rank histograms were constructed by counting the number of training examples with a certain rank, as shown in Fig. 1. Based on the histograms, we selected the most frequently occurring rank as the number of CPD components to extract. This was clearly $R = 1$ for HH_Tensors. In case of W_Tensors the rank value was clearly 3 in frequency mode, but more distributed in other modes. Finally, we chose $R = 3$, as further increasing the rank gave only small *relerr* reductions (until $R = 7$).

The signatures resulting from the tensor decomposition were used as features to perform the classification.

D. Classification

Five classifiers were trained to perform the NCES detection: a K-Nearest Neighbour classifier (KNN) with K=3, a Backpropagation Neural Network (NNBP), a Naïve Bayes Classifier (BAYES), a linear Support Vector Machine (SVM) and a Radial Basis SVM (SVMRB).

The classification was done for each patient individually. The training set for each patient was assembled with all EEG epochs of the first seizure (= positive class) and the same number of non-seizure EEG epochs prior to the first seizure (= negative class). The Classification was performed in two ways: (1) with each signature of the different modes (channel, time, frequency) separately, (2) with all signatures assembled.

The classifiers performance was evaluated in terms of sensitivity, accuracy and false positive rate. The sensitivity can be expressed as,

$$Sen = \frac{TP}{TP + FN} \tag{12}$$

The accuracy is defined as,

$$Acc = \frac{TP + TN}{TP + FP + TN + FN} \tag{13}$$

The false positive rate denotes the Type I error ratio (false epochs classified as positives) is defined as

$$FPR = \frac{FP}{FP + TN} \tag{14}$$

Where TP is the number of seizure epochs correctly detected, FP is the number of false alarms, TN is the number of seizure free epochs correctly detected and FN is the number of missed seizure epochs.

III. Results and Discussion

The results obtained from the individual signatures' classification are shown in Fig. 2. The NCES detection sensitivity using HH_Tensors signatures was higher compared to the one obtained with W_Tensors signatures. This can be explained by the fact that HH_Tensors are closer to rank one, capturing the seizure with R=1. Then, all features obtained for these tensors are relevant for the seizure classification. However, for W_Tensors with R=3, not all terms represent seizure activity; therefore, some of the signatures are not relevant for the classification. Different mother wavelets and different frequency ranges (e.g. 1-30Hz [6], [4]) were also tested for W_Tensors

ISBN 978-0-9928626-7-1 © EURASIP 2017

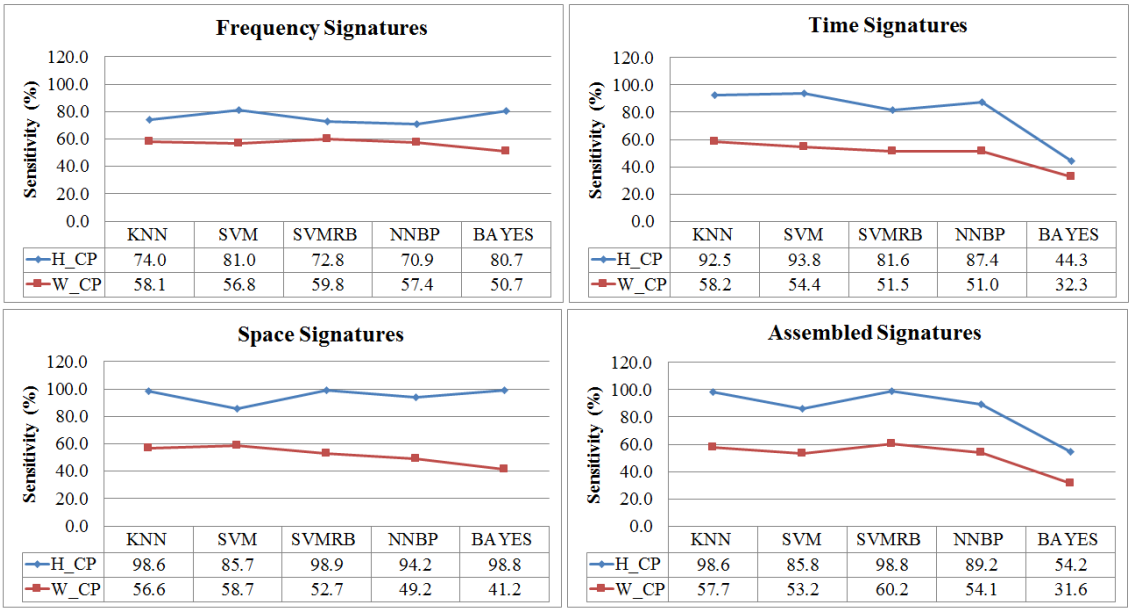

Fig. 2. Classification sensitivity results for individual and assembled signatures. H_CP and W_CP are the signatures obtained from HH_Tensors and W_Tensors CPD respectively.

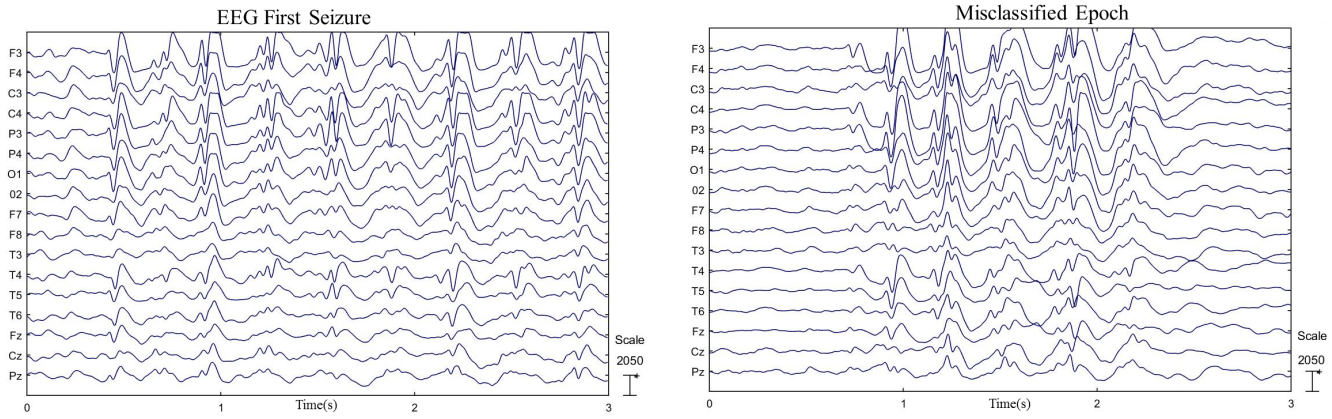

Fig. 3. Subject 10 first seizure and a negative epoch misclassified as positive due to a paroxysmal burst.

representation, but without significant improvement of the results.

We further discuss the performance of HH_Tensors representation. Comparing the classification performance of the individual signatures in the three different modes, we see that Space signatures achieved the best results, closely followed by Time signatures. The sensitivity of the KNN and SVM classifiers using these signatures were over 90% with 0.1 and $7 * 10^{-2}$ false detections per hour, respectively, both outperforming Frequency signatures.

This is not entirely surprising, as in an initial analysis comparing the probability distribution of the obtained signature values for both W_Tensors and HH_Tensors, we observed that the values obtained by HH_Tensors Space and Time signatures separate better between seizure and non-seizure epochs. This behaviour is related to the resemblance between the EEG patterns from the subjects' first seizure and some segments marked as seizure-free. This is caused by the presence of a large number of spikes or long paroxysms that resemble a seizure. Fig. 3 shows an example of this phenomenon.These paroxystic segments, according to medical convention, are too brief to be classified as seizures. Yet, the possibility of predicting seizures with these detections can be interesting, since this activity can be a seizure precursor [13]. Another reason for the FP detections is due to electrode artefacts on seizure-free epochs. Interestingly, both paroxysms and artifacts affect Frequency signatures more than Space and Time signatures.

As HH_Tensors Space signatures achieved the best sensitivity, we further analyse its performance in combination with different classifiers. The highest average sensitivity was achieved by KNN, SVMRB and BAYES classifiers (see

ISBN 978-0-9928626-7-1

Fig.2). The accuracy values for these classifiers range between $98.6 - 99.0\%$. In terms of false positive rate, KNN obtained 0.1 false detections per hour. Since, as explained above, the probability distribution of the Space signatures for seizure and seizure-free epochs were clearly separated, and given that the KNN classifier bases its decisions on distance measures in a small neighborhood of similar objects, this performance is expected. The minimum number of false detections per hour was achieved by SVMRB and BAYES with $7*10^{-2}$. However, the BAYES classifier obtained a very low sensitivity of 44.3% for the Time signatures. Naïve Bayes classifier assumes statistical independence of the data. A post-hoc analysis revealed that mutual information estimates for the Time signatures often take values over 0.7. This suggests that Time signatures are not statistically independent, and could explain why BAYES classifier does not perform properly for them.

Although sensitivity and accuracy values achieved by NNBP for the Space signatures are over the 90%, it has a high false positive rate and it shows relatively low performance for the other signatures. The used training datasets are small and neural networks needs large training datasets to improve the classification results.

Finally, SVMRB outperformed SVM. In fact, this is the case for all signatures, except for Time signatures. This suggests that the difference between seizure and non-seizure epochs is best described in terms of a non-linear function of the signatures.

The assembled signatures performed similarly to the HH_Tensors space signatures in terms of sensitivity and accuracy. The best classifiers for this approach are KNN and SMVRB, both with a sensitivity and accuracy values of 98.7 and 98.9%, respectively. The number of false detections per hour obtained using the assembled signatures (for KNN $9 * 10 - 2$ and for SVMRB $7 * 10^{-2}$) are similar to the ones achieved by the HH_Tensors Space signatures. The missed positive epochs for the assembled training correspond mainly to the beginnings and endings of seizures, where the seizure activity is less clear (mainly in subjects 2 and 12).

IV. Conclusion

This study proposes a method for NCES detection that applies for the first time HHT and multiway data analysis for this kind of seizures.

From the two analysed tensor sets, the results obtained for the one built with HHT are superior to the one obtained with WT. The $frequency \times energy \times time$ distribution offered by HHT captures the NCES data in a tensor close to R=1. This turns all signatures obtained from HH_Tensors decomposition in relevant features to perform the NCES detection, with high performance.

From all performed analyses, HH_Tensors Space signatures demonstrate to be the best feature to classify between seizure and non-seizure epochs. These signatures obtained sensitivity and accuracy values over 95% for the best classifiers evaluated, KNN and SVMRB.

We conclude that multiway analysis of EEG data by means of HHT and low rank tensor decompositions, in combination with an appropriate choice of classifier is an effective way to detect non-convulsive epileptic seizures.

References

[1] J. Wilson and H. Nordal, "Eeg in connection with coma." *Tidsskrift for den Norske laegeforening: tidsskrift for praktisk medicin, ny raekke*, vol. 133, no. 1, pp. 53–57, 2013.

[2] A. Q. Ansari and P. Sharma, "A review on automated detection of non-convulsive seizures using eeg," in *Computational Intelligence & Communication Technology (CICT), 2016 Second International Conference on*. IEEE, 2016, pp. 283–286.

[3] H. Liang, S. L. Bressler, R. Desimone, and P. Fries, "Empirical mode decomposition: a method for analyzing neural data," *Neurocomputing*, vol. 65, pp. 801–807, 2005.

[4] B. Hunyadi, D. Camps, L. Sorber, W. Van Paesschen, M. De Vos, S. Van Huffel, and L. De Lathauwer, "Block term decomposition for modelling epileptic seizures," *EURASIP Journal on Advances in Signal Processing*, vol. 2014, no. 1, p. 139, 2014.

[5] C. Guerrero-Mosquera, M. Verleysen, and A. N. Vazquez, "Eeg feature selection using mutual information and support vector machine: A comparative analysis," in *Engineering in Medicine and Biology Society (EMBC), 2010 Annual International Conference of the IEEE*. IEEE, 2010, pp. 4946–4949.

[6] E. Acar, C. Aykut-Bingol, H. Bingol, R. Bro, and B. Yener, "Multiway analysis of epilepsy tensors," *Bioinformatics*, vol. 23, no. 13, pp. 10–18, 2007.

[7] M. Leitinger, S. Beniczky, A. Rohracher, E. Gardella, G. Kalss, E. Qerama, J. Höfler, A. H. Lindberg-Larsen, G. Kuchukhidze, J. Dobesberger *et al.*, "Salzburg consensus criteria for non-convulsive status epilepticus–approach to clinical application," *Epilepsy & Behavior*, vol. 49, pp. 158–163, 2015.

[8] N. E. Huang, Z. Shen, S. R. Long, M. C. Wu, H. H. Shih, Q. Zheng, N.-C. Yen, C. C. Tung, and H. H. Liu, "The empirical mode decomposition and the hilbert spectrum for nonlinear and non-stationary time series analysis," in *Proceedings of the Royal Society of London A: Mathematical, Physical and Engineering Sciences*, vol. 454, no. 1971. The Royal Society, 1998, pp. 903–995.

[9] N.-F. Chang, T.-C. Chen, C.-Y. Chiang, and L.-G. Chen, "On-line empirical mode decomposition biomedical microprocessor for hilbert huang transform," in *Biomedical Circuits and Systems Conference (BioCAS), 2011 IEEE*. IEEE, 2011, pp. 420–423.

[10] M. Sørensen and L. De Lathauwer, "Tensor decompositions with block-toeplitz structure and applications in signal processing," in *Signals, Systems and Computers (ASILOMAR), 2011 Conference Record of the Forty Fifth Asilomar Conference on*. IEEE, 2011, pp. 454–458.

[11] N. Vervliet, O. Debals, L. Sorber, M. Van Barel, and L. De Lathauwer, "Tensorlab 3.0," *available online, URL: www. tensorlab. net*, 2016.

[12] M. Ishteva, P.-A. Absil, S. Van Huffel, and L. De Lathauwer, "Best low multilinear rank approximation of higher-order tensors, based on the riemannian trust-region scheme," *SIAM Journal on Matrix Analysis and Applications*, vol. 32, no. 1, pp. 115–135, 2011.

[13] E. M. Donnelly and A. S. Blum, "Focal and generalized slowing, coma, and brain death," in *The Clinical Neurophysiology Primer*. Springer, 2007, pp. 127–140.

ISBN 978-0-9928626-7-1 © EURASIP 2017